Int. J. Electrochem. Sci., 6 **(2011)** 3316 - 3332

International Journal of
ELECTROCHEMICAL
SCIENCE
www.electrochemsci.org

Nanotube Arrays as Photoanodes for Dye Sensitized Solar Cells Using Metal Phthalocyanine Dyes

Nada F. Atta, Hatem M.A. Amin, Mohamed W. Khalil, Ahmed Galal[*]

Department of Chemistry, Faculty of Science, Cairo University, Postal Code 12613, Giza, Egypt
[*]E-mail: galalh@sti.sci.eg

Received: 8 June 2011 / *Accepted:* 3 July 2011 / *Published:* 1 August 2011

A highly ordered TiO_2 nanotubes (NT_s) array was grown on Ti substrate by anodization method in HF-H_3PO_4 electrolyte. The morphology and microstructure of TiO_2 NT_s were investigated by scanning probe microscope (SPM), scanning electron microscope (SEM) and X-ray diffraction (XRD). It was found that anatase phase of TiO_2 prevailed with an average inner pore diameter of about 110 nm. The applicability of TiO_2 NT_s arrays to dye sensitized solar cells ($DSSC_s$) using different metal phthalocyanine dyes was studied in dark and under illumination. The photoelectrochemical properties of the prepared TiO_2 electrodes under different conditions were investigated using I-V characteristic curves. Interesting results were obtained using cobalt phthalocyanine (CoPC) dye sensitized nanotubular TiO_2 solar cell under optimized conditions which showed good conversion efficiency (0.17 %) under illumination of 100 mW cm^{-2} with good stability for many turnovers.

Keywords: TiO_2-nanotubes; photoelectrochemistry; DSSC; SPM; SEM; XRD.

1. INTRODUCTION

Solar-energy conversion and electric-energy storage are becoming key techniques towards issues on energy crisis and sustainable use. For the solar-energy conversion, as mostly by the form of solar cell, dye-sensitized solar cells ($DSSC_s$) with nanocrystalline TiO_2, dye molecules, and electrolytes are recently developed for light harvesting [1, 2]. Dye-sensitized solar cells ($DSSC_s$) have become the most promising alternative to the conventional silicon-based solar cells. In a widely adopted nanoparticulate titania (TiO_2) based DSSC, the dye sensitizer adsorbs photons to excite electrons to be injected to the conduction band of titania, which then transport to a current collector to generate a photocurrent. The macroscopic assembly of the titania nanoparticles, which served as a photoanode, determines to a great extent the efficiency of a DSSC [3, 4]. The mesoporosity and

nanocrystallinity of the semiconductor are important for the adsorption of a large amount of dye molecules [5].

TiO_2 nanotubes are also found to contribute beneficially to the high efficiency due mainly to an improved electron transfer through the titania photoanode to the current collector. TiO_2 is a widely used semiconductor due to its high stability, favorable bandgap energy, abundant availability, and inexpensive cost [6]. Because TiO_2 is a large bandgap semiconductor (bandgap = 3.1-3.2 eV), it absorbs only solar light in the UV region. The major problem is that only about 4-5 % of the solar spectrum falls in this UV range. To improve the photocatalytic efficiency, researchers have adopted different strategies such as changing the electrical properties of TiO_2 by varying the crystalline size [7]; doping TiO_2 with metal/nonmetal ions in order to induce red shift to the bandgap [8]. Nanostructured titania was prepared in the form of several morphologies for example, nanoparticle [9], nanorod [10], and nanotube [11], which can be fabricated by sol–gel method [12], hydrothermal synthesis in an alkaline solution [13] and electrochemical anodization in a solution containing fluoride ion [14]. Those nanostructures are expected to be applied for photoanodes in photoelectrochemical systems [15] and dye-sensitized solar cells [16]. Among them, we focused on titania nanotube or its related structure by anodization. The nanotube related structure can be fabricated on the bulky substrate; therefore an electron produced at the surface of nanotube can be directly transported into a current collector without large point contact resistance which occurred at the boundary between nanoparticles.

The morphology and microstructure of the TiO_2 layer depend greatly on the electrolyzing parameters and electrolyte components [17]. H. Wang et al. [18] successfully employed the anodic oxidation method to the direct growth of immobilized TiO_2 nanowires on titanium foil in ethylene glycol electrolyte solution contained HF and water. The influence of porous morphology on the microstructure and optical properties of TiO_2 films prepared by different sol concentrations and calcination temperatures was investigated by R. Sathyamoorthy et al. [19]. M. Pedeferri et al. [20] aimed to evaluate the effects of titanium anodic oxidation in a sulphuric acid electrolyte on the crystallinity of the oxide layer and to adjust the process parameters, in order to maximize the TiO_2 crystalline phase, especially for what concerns the anatase form.

The most successful charge-transfer sensitizers employed so far in $DSSC_s$ are ruthenium (II) polypyridyl complexes. They produced solar energy-to-electricity conversion efficiencies up to 11% under AM 1.5 irradiation and stable operation for millions of turnovers [1]. In spite of this, the main drawbacks of these sensitizers are the lack of absorption in the red region of the visible spectrum and also relatively low molar extinction coefficient above 600 nm. In contrast, phthalocyanines possess intense absorption bands in the near-IR region and are known for their excellent chemical, photo and thermal stability; and have appropriate redox properties for sensitization of wide bandgap semiconductors, e.g., TiO_2, rendering them attractive for DSSC applications [21]. Several groups have tested phthalocyanines as sensitizers for wide bandgap oxide semiconductors. Although they all have been reported small power conversion efficiencies [22], the low efficiency of cells incorporating phthalocyanines appears to be due to aggregation, solubility and lack of directionality in the excited state.

In the present work, titania nanotube arrays were deposited on Ti substrate by direct oxidizing the Ti substrate in HF- H_3PO_4 solution. Characterization of TiO_2 NT_s electrodes prepared under different conditions was also reported. The applicability of such nanotube arrays as photoanodes to $DSSC_s$ using different metal phthalocyanine dyes was studied. Good results were obtained using CoPC dye sensitized TiO_2 NT_s solar cell compared to other results obtained in the literature. So, preparing and examining CoPC dye sensitized nanotubular TiO_2 photoanode under optimized conditions showed better conversion efficiency under illumination of 100 mW cm^{-2} (0.17 %) compared to dark conditions (0.08 %).

2. EXPERIMENTAL

2.1. Preparation of TiO_2 nanotube arrays

The constant potential anodization process was used to fabricate the TiO_2 NT_s electrodes. Prior to anodization, the Ti rod electrode was first mechanically polished with different abrasive papers and Alumina (2 μm) /water slurry on BUEHLER pads and cleaned in ethanol, acetone and followed by chemical polishing in strong acidic solution of HF (3.3 M)-HNO_3 (5.6 M) for 15 seconds to form a fresh smooth surface. Ti electrode was then rinsed by water and dried in air at room temperature. The TiO_2 NT_s electrode was fabricated in a cylindrical plastic cell equipped with a regulated direct current (DC) power supply with a two-electrode configuration, in which the pre-treated Ti electrode was used as a working electrode for an anode role and a platinum sheet foil acting as a counter electrode. The distance between Ti electrode and Pt electrode was fixed at 3.5 cm. Different mole fractions of the electrolyte HF (0.09 – 0.41) and of the H_3PO_4 (0.91-0.59) were used. A potential (5 – 25 V) was used and anodization duration (20 – 100 minutes) was applied in this study. After anodization, the electrode was thoroughly rinsed in distilled water and subsequently in acetone, and finally dried in air. Anodized Ti electrode was annealed in an oven at 105˚C for 12 hours. Finally, the electrode was calcinated at different temperatures (350- 650˚C) for different times (0.5– 4 hours). At the final stage, well-ordered TiO_2 NT_s were fabricated under optimized conditions.

2.2. Characterization of TiO_2 NT_s array electrode

The surface morphology of the prepared TiO_2 NT_s film was examined using a scanning probe microscope (SPM-9600, SHIMADZU Corporation, Japan) operated on the contact mode. Scanning electron microscope (SEM), Philibs XL 30 instrument, was also used to investigate the morphology of TiO_2 NT_s films. Samples investigated by SEM and SPM were prepared as previously mentioned in the experimental section. The SEM images were processed with a personal computer connected to the SEM. The crystalline structure and the phase purity of TiO_2 samples were analyzed by X-ray diffraction (PANalytical X'pert PRo XRD instrument with Cu K_α radiation operating at 45 kV and 40 mA). XRD patterns of TiO_2 films were collected at a scan rate of 4º /min in the 2θ range of 20º – 80º. Electrochemical impedance spectroscopy (EIS) has been widely employed to study the kinetics of

electrochemical and photoelectrochemical processes occurring in the dye sensitized solar cells. In this study, impedance spectrum analysis had been applied to explore the electric conductivity of TiO_2 electrode [1] under open-circuit potential (OCP) over the frequency range of 0.1 Hz - 100 kHz and ac-voltage amplitude of 10 mV. One of the factors affecting the photoelectrochemical and chemical processes studied by EIS was the effect of illumination. The EIS measurements for the TiO_2 NT_s electrode prepared under optimum conditions were performed at room temperature in 10^{-3} M dye/1M H_2SO_4 solution in dark and under illumination. The EIS measurements were carried out with Gamry-750 system and a lock-in-amplifier that are connected to a personal computer. The data analysis software was provided with the instrument and applied non-linear least square fitting with Levenberg-Marquadt algorithm. The best fitting values calculated from the equivalent circuit for the impedance data were reported.

2.3. Photoelectrochemical measurements

I-V characteristics of the electrodes prepared at different conditions were recorded in a dye electrolyte at room temperature using Gamry-750 system in dark and under illumination of 100 mW cm^{-2}. The conversion efficiency (η) and the fill factor (FF) of the prepared solar cell systems were calculated from I-V parameters.

3. RESULTS AND DISCUSSION

The factors affecting morphology, pore size and crystallographic structure of TiO_2-NT_s were studied in order to achieve the optimum conditions for TiO_2-NT_s electrode for solar cell application. The pore size of TiO_2-NT_s can be tuned as required by changing the synthesis parameters [23]. The effect of the dye as a sensitizer in the $DSSC_s$ was also explained. The effect of illumination on the performance of the solar cell was studied.

3.1. Effect of anodization voltage

Anodization voltage strongly affects the spacing and pore size of TiO_2-NT_s [24] because the electrochemical etching rate depends on the anodization potential. The nanotube formation process includes electrochemical etching of Ti and chemical dissolution of oxide formed. The nanotube depth increases till the electrochemical etching rate becomes equal to the chemical dissolution of the top surface of the nanotubes. Higher anodization voltages increase the oxidation and field assisted dissolution hence a greater nanotube layer thickness can be formed before equilibrating with the chemical dissolution. Fig. 1 shows the SEM micrographs of TiO_2 NT_s obtained by anodization for 40 minutes in 0.15M HF + 0.5M H_3PO_4 aqueous solution at room temperature at different cell voltage (5, 15, 20 and 25 V, respectively) then annealed and calcinated at 450˚C for 2 hours. The corresponding

average pore diameter of TiO_2-NT_s as a function of the anodization cell voltage is reported and shown in Fig. 1E.

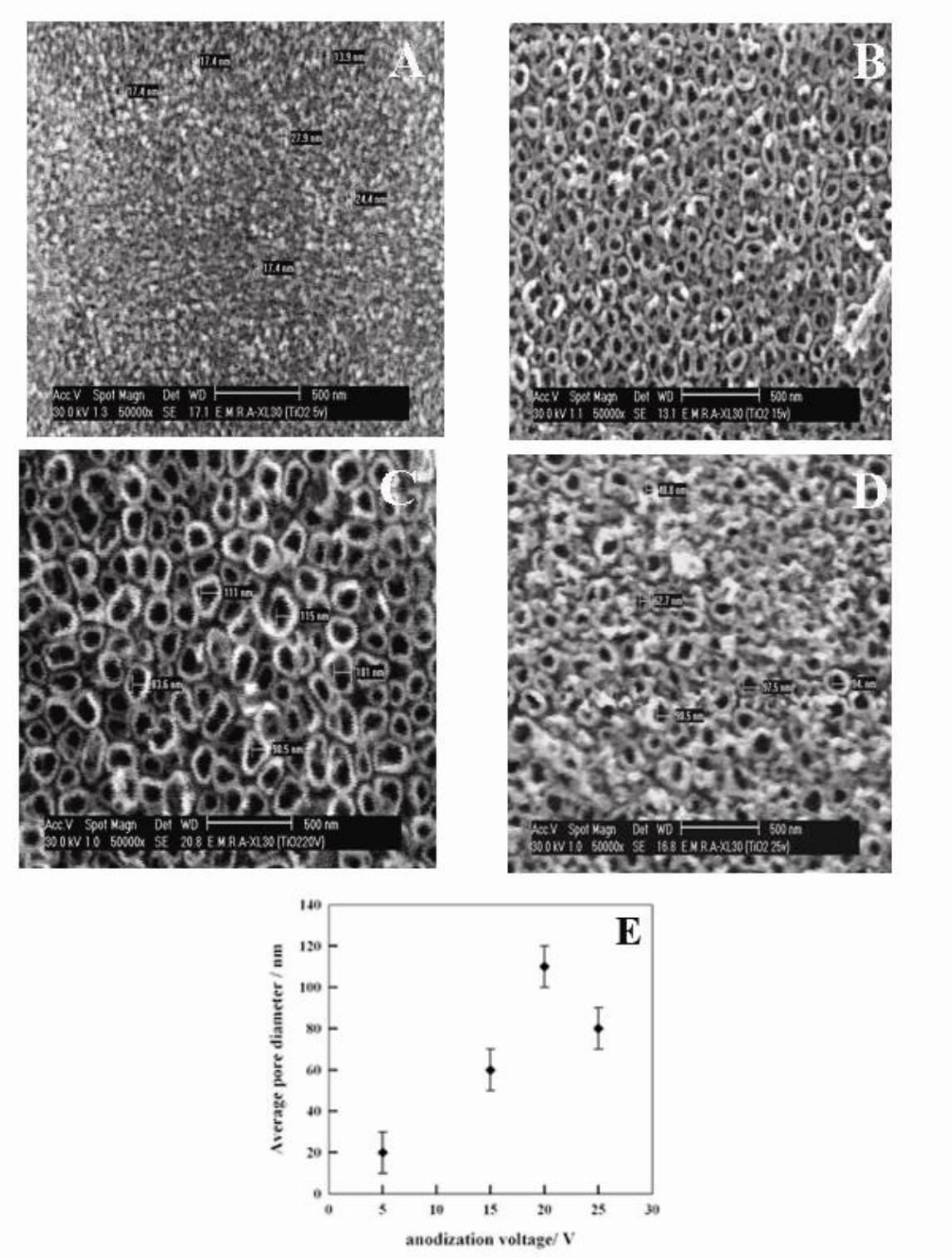

Figure 1. SEM images of TiO_2 NT_s prepared at different anodization potentials in 0.15M HF + 0.5M H_3PO_4 for 40 min. and then annealed and calcinated at 450˚C for 2 hours, A: 5V, B: 10V, C: 15V, D: 20V, E: plot of the average pore diameter as a function of anodization voltage.

By increasing the anodization voltage from 5 to 20 V, an increase in the average pore diameter from about 20 to 110 nm, respectively, was observed. While in case of anodization voltage of 25V, the pore diameter decreases to about 80 nm. Such results are in a good agreement with published results [23, 24]. SEM analysis leads to the conclusion that the anodization voltage of 20V gives the largest pore diameter and interspacing. Depending on the anodization conditions, TiO_2 can be prepared in amorphous or crystalline form (anatase, rutile or a mixture of anatase and rutile) [24]. Anatase is the main phase in the prepared TiO_2 film and the crystallinity increases as the anodization voltage increases as observed from XRD data.

The photovoltammetry can be used to evaluate both of the electrochemical behavior with light off and the photoelectrochemical behavior with light on under the same experimental conditions of TiO_2 electrodes [25]. The performance parameters of DSSC based on TiO_2 NT_s electrode prepared under different anodization voltages were obtained from I-V characteristic curves and are tabulated in table 1 where 10^{-3} M CoPC dye solution and 100 mW cm^{-2} illuminations were applied. From I-V data, we found that the conversion efficiency changes as the anodization voltage changes which might be due to change of the pore size of TiO_2-NT_s. The greater the pore size and the greater the amount of dye absorbed, the more enhanced the electron transfer process with better conversion efficiency.

Table 1. I-V characteristics of TiO_2 NT_s electrodes prepared under different conditions and then annealed at 105˚C for 12 hours and calcinated at 450˚C for 2 hours and tested in dye solution under illumination of 100 mW cm^{-2}.

Anodization voltage / V	**I_{sc}/ A**	**V_{oc}/ V**	**FF**	**% η**
10	**6.99×10^{-4}**	**0.25**	**0.68**	**0.12**
15	**4.45×10^{-3}**	**0.20**	**0.15**	**0.14**
20	**7.97×10^{-4}**	**0.21**	**0.97**	**0.16**
25	**6.01×10^{-4}**	**0.28**	**0.38**	**0.06**
Anodization duration/ min.				
20	**5.39×10^{-4}**	**0.18**	**0.70**	**0.07**
40	**7.32×10^{-4}**	**0.19**	**0.96**	**0.13**
60	**7.53×10^{-4}**	**0.21**	**0.06**	**0.01**
100	**7.21×10^{-4}**	**0.20**	**0.30**	**0.04**

3.2. Effect of anodization duration

Fig. 2 shows the SEM micrographs of TiO-$_2NT_s$ prepared at 20V in 0.5M H_3PO_4 + 0.15M HF for 20, 40 and 100 minutes, respectively, and then annealed at 105˚C for 12 hours and calcinated at 450˚C for 2 hours. The pore size of TiO_2-NT_s depends on the rate of both oxide formation and oxide dissolution. Both processes affected by anodization duration. At the first stages of anodization, the

pore entrance is not affected by electric field assisted dissolution and hence remains relatively narrow, while the electric field distribution in the curved bottom surface at the pore causes pore widening as well as deepening the pore [26]. The result is a multiporous TiO_2 as observed after about 20 min. (see Fig. 2A). As the Ti-O bond energy is high, bare metallic regions can initially exist between pores. As the pores become deeper, the electric field in these regions increases enhancing oxide growth and oxide dissolution hence simultaneously with the pores well-defined inter-pore voids start forming. Thereafter, both voids and tubes grow simultaneously [27]. This is observed after 40 minutes of anodization (see Fig. 2B) and after long time of anodization (100 min.), the pore size decreases because the voids exceed the tubes in size (see Fig. 2C).

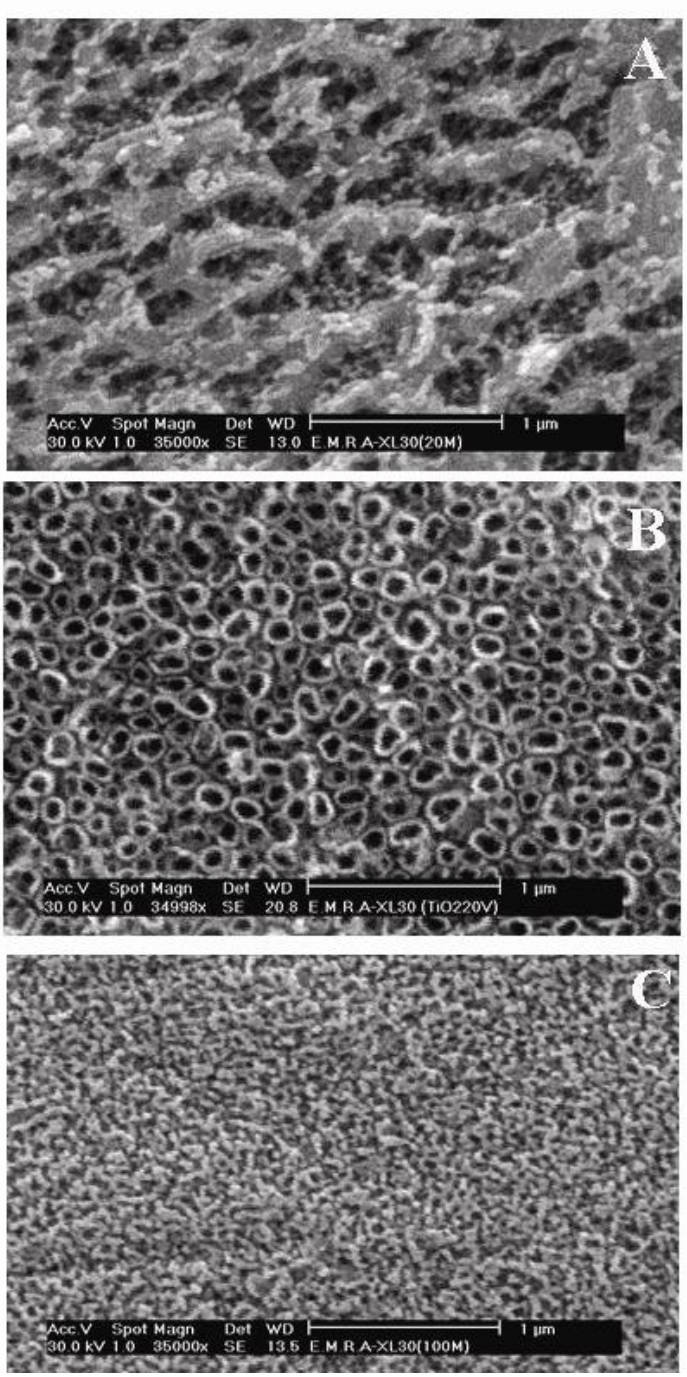

Figure 2. SEM images of TiO_2 NT_s prepared at 20V in 0.15M HF + 0.5M H_3PO_4 for different times, (A) 20 min., (B) 40 min., (C) 100 min., and then annealed and calcinated at 450˚C for 2 hours.

The change of the conversion efficiency of the solar cells based on TiO_2 electrodes prepared under different times of anodization is related to the morphology of TiO_2-NT_s as shown in table 1. Mende and Grätzel [28] showed that if the pores of TiO_2-NT_s are not completely filled with dye, it leads to lower current densities and poorer performance of the cell under illumination. So, as the pore size increases, there is a better chance to be completely filled with dye and hence the efficiency and performance of the cell increase. Such conclusions agree with our results. The conversion efficiency percent (%η) reaches its optimum value of 0.13 % after 40 min. of anodization under illumination conditions of 100 mW cm^{-2} and under the previously mentioned preparation conditions.

3.3. Effect of HF concentration

SEM images of TiO_2 prepared at 20V for 40 min. in H_3PO_4 electrolyte containing different mole fractions of HF (0.09 to 0.31) and annealed in an oven at 105˚C for 12 hours then calcinated at 450˚C for 2 hours are shown in Fig. 3.

The electrochemical etching rate during TiO_2 formation depends on the concentration of electrolyte. The chemical dissolution rate is determined by fluoride ion (F^-) concentration and solution pH. With increase in F^- and H^+ concentrations, chemical dissolution increases and hence the pore diameter increases reaching the largest pore size (110 nm) at 0.23 mole fraction of HF but at higher mole fraction of HF, random TiO_2 film is formed extending out from the pores. Recent investigations have shown that only in a certain F^- concentration range nanotubes array could be achieved [27] and it is agreed and confirmed our results. Constant potential anodization in H_3PO_4 electrolyte containing 0.09 mole fraction of HF, or less, produces disordered and spongy-like porous TiO_2 films. The nanotubular geometry of TiO_2 is preferred as it provides a higher interfacial reaction area and better electron transfer.

3.4. Effect of calcination temperature

The morphology and pore size of TiO_2-NT_s are strongly affected by the thermal post-treatment of the prepared surfaces. Calcination temperature affects the pore diameter and interspacing in the prepared TiO_2-NT_s. It also affects the homogeneous distribution and ordering of the pores. Lower calcination temperatures (350˚C or less) resulted in formation of pores with smaller sizes and non-homogeneous diameters. Moreover, the surface of TiO_2 tends to be disordered and compact in some areas. At 450˚C calcination temperature, the nanotubular structure is homogeneous and ordered. The higher calcination temperatures used (550˚C or more) lead to disordered pores and non-homogeneous pore sizes. Some regions with spongy-like structure have been noticed from the SEM image. The photoelectrochemical behavior of TiO_2-NT_s prepared and calcinated at different temperatures was examined in presence of CoPC dye under illumination. Cell performance parameters are reported in table 2. The calcination temperature affects the morphology and nanotubular structure of TiO_2. Also, the pore size and structure of TiO_2-NT_s influence the electron transfer and dye absorption processes in this system and consequently affects on the conversion efficiency of TiO_2-NT_s and hence the

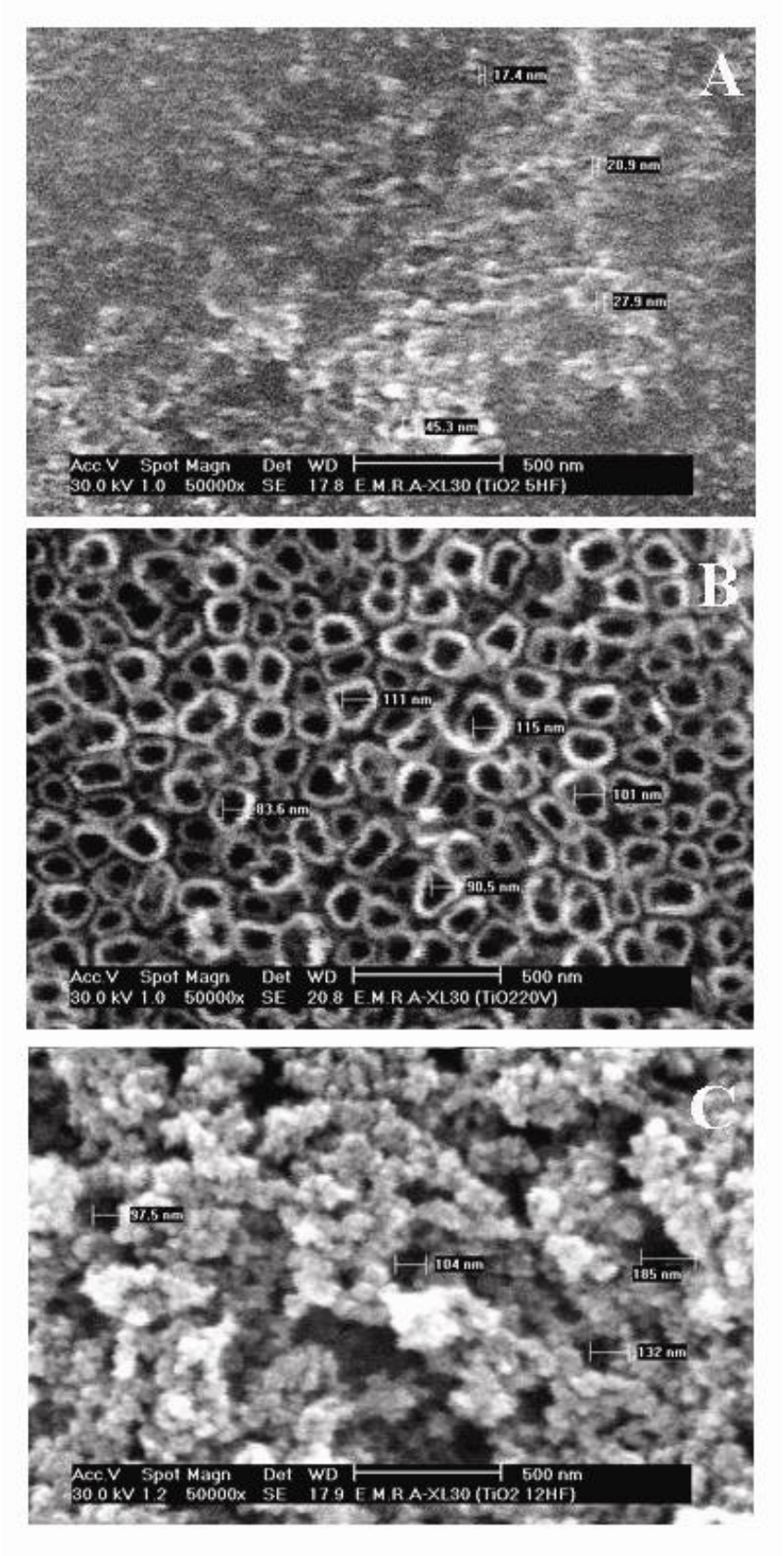

Figure 3. SEM images of TiO_2 prepared at 20V in H_3PO_4 electrolytes containing different mole fractions of HF for 40 min. and annealed then calcinated at 450˚C for 2 hours, A: 0.09, B: 0.23, C: 0.31 mole fraction of HF.

performance of TiO_2 solar cell. As the pore size increases, the conversion efficiency increases because the nanotubular structure has better electron transfer and large surface area than planar bulk film [29]. The optimum calcination temperature with the highest conversion efficiency of TiO_2 solar cell prepared here is 450˚C. This result fits with the SEM result (Fig. not included) where TiO_2-NT_s electrode calcinated at 450˚C showed the largest pore size and interspacing and hence the best conversion efficiency obtained under the studied conditions.

Table 2. I-V characteristics of TiO_2 NT_s electrodes prepared by anodization at 20 V in 0.15M HF + 0.5M H_3PO_4 for 40 min. and then annealed and calcinated under different conditions and tested in CoPC dye electrolyte under illumination of 100 mW cm^{-2}.

Calcination Temperature/ ˚C	**I_{sc}/ A**	**V_{oc}/ V**	**FF**	**% η**
350	**4.63×10^{-4}**	**0.17**	**0.99**	**0.08**
450	**9.01×10^{-4}**	**0.16**	**0.98**	**0.15**
550	**7.34×10^{-4}**	**0.20**	**0.48**	**0.07**
650	**5.52×10^{-4}**	**0.23**	**0.30**	**0.04**
Calcination duration/ hours				
0.5	**4.55×10^{-4}**	**0.18**	**0.31**	**0.03**
1	**7.11×10^{-4}**	**0.14**	**0.42**	**0.04**
2	**8.01×10^{-4}**	**0.18**	**0.93**	**0.13**
4	**7.66×10^{-4}**	**0.17**	**0.24**	**0.03**

3.5. Effect of calcination duration

Calcination duration is another factor affecting the behavior, crystal phase and morphology of TiO_2. Two hours of calcination was found to be optimum time to get the largest and the more homogenous pore size. Calcination duration affects the crystallization process. XRD measurements were used to determine the crystal phase behavior of TiO_2 NT_s electrode. XRD patterns of TiO_2-NT_s prepared by anodization at 20V in 0.5M H_3PO_4+0.15M HF for 40 min. and then TiO_2 annealed and calcinated at 450˚C for different periods of time are shown in Fig. 4.

XRD results are in a good agreement with the theoretical data in the ICCD card. For TiO_2 electrode prepared and analyzed without calcination, an amorphous phase is dominant and no TiO_2 peaks appeared. This emphasizes the role of calcination duration on the formation of TiO_2. After the TiO_2 electrode was calcinated at 450 ˚C for different times, an anatase phase, with tetragonal structure, (2θ~25.3˚ for (101) anatase) appeared and no rutile phase exists. Such results agree with the previous work [30]. The crystallinity increases as the calcination duration increases reaching a higher crystallinity after 2 hours of calcination. The crystallinity of TiO_2 calcinated for 4 hours is nearly the

same as that calcinated at 2 hours but with smaller pore size of TiO_2. Ti peaks with hexagonal structure appear clearly-underlying matrix. Very small peaks correspond to the rutile phase appears which is not dominant in the XRD patterns. So, anatase phase of TiO_2 prevails under the mentioned conditions of preparation.

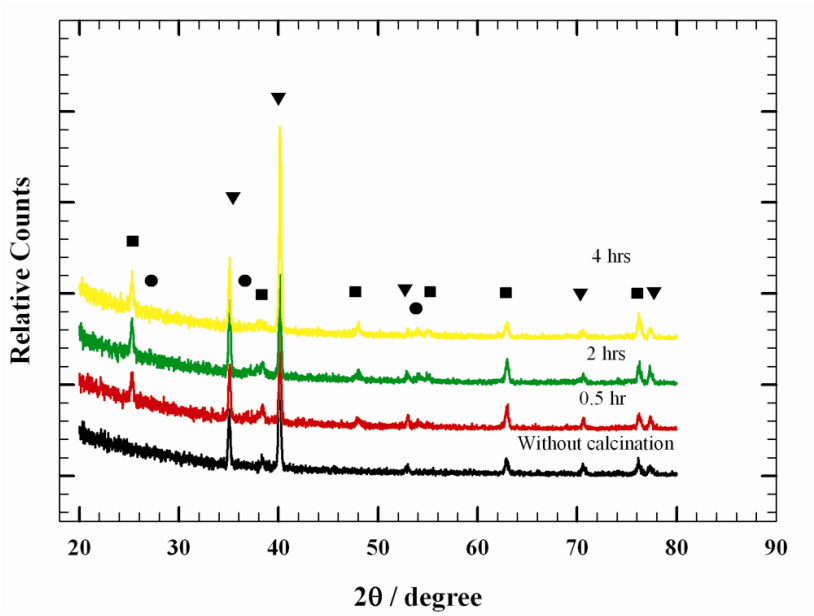

Figure 4. XRD patterns of TiO_2 prepared at 20 V in 0.15M HF + 0.5M H_3PO_4 for 40 min. and then annealed and calcinated at 450˚C for different times.

The photoelectrochemical response of DSSC based on TiO_2 electrode calcinated at different times was investigated in CoPC dye solution under illumination. The fill factor and conversion efficiency values are calculated from I-V curves and reported in table 2. As the anodization time increases from 0.5 to 2 hours, the conversion efficiency increases from 0.03% to 0.13%, respectively, under illumination, then the conversion efficiency decreases again to 0.03% after 4 hours calcination. Such results are related to the corresponding morphology and pore size of TiO_2-NT_s and the amount of dye absorbed in the pores.

Scanning probe microscope (SPM) was used to investigate the morphological characteristics of TiO_2-NT_s electrode prepared under the experimentally optimized conditions: 20V anodization voltage for 40 min. in 0.5M H_3PO_4 + 0.15M HF and annealing at 105˚C for 12 hours then calcination at 450˚C for 2 hours. Fig. 5 is the SPM picture (surface plot) of TiO_2-NT_s in which TiO_2 film consists of interconnected pores.

3.6. Effect of the dye

The dye used in the solar cell has an effect on its performance and efficiency. Phthalocyanines have intense absorption in the red region above 600 nm. They also have excellent chemical, photo and

heat stabilities; moreover, they have the energy levels that match that of TiO_2. All these properties make phthalocyanines complementary to ruthenium (II) polypyridyl complexes. TiO_2-NT_s electrode was prepared under the experimentally optimized conditions mentioned above. The prepared electrode was then tested in 10^{-3}M of different dyes namely; CoPC, CuPC and NiPC, respectively, under illumination and their I-V characteristic curves are shown in Fig. 6. The conversion efficiency percent of solar cell based on TiO_2-NT_s tested in CoPC, CuPC and NiPC dyes are 0.17, 0.12 and 0.06%, respectively, under illumination. So, CoPC dye showed better conversion efficiency under the studied conditions compared to the other dyes used.

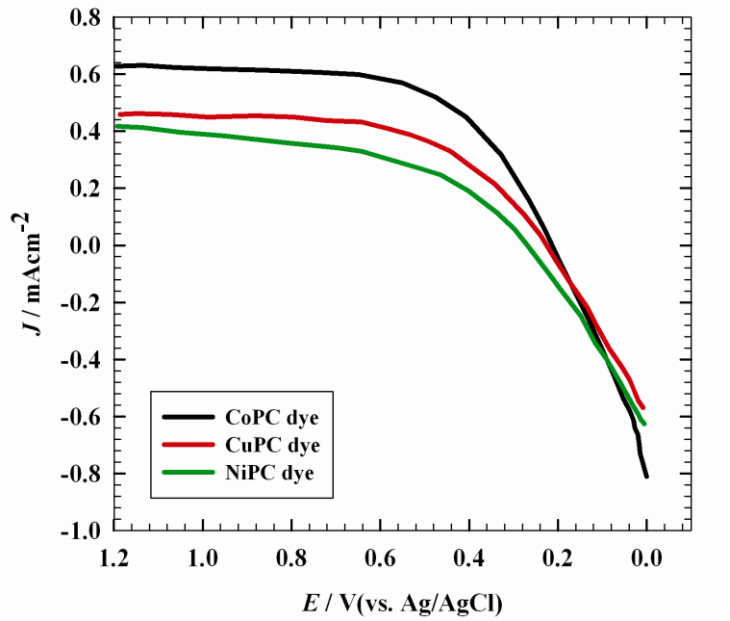

Figure 6. I-V curves of TiO_2 electrodes prepared by constant potential anodization at 20 V in 0.15M HF + 0.5M H_3PO_4 for 40 min. and then annealed and calcinated at 450˚C for 2 hours and tested in different dyes under illumination of 100 mW cm^{-2}.

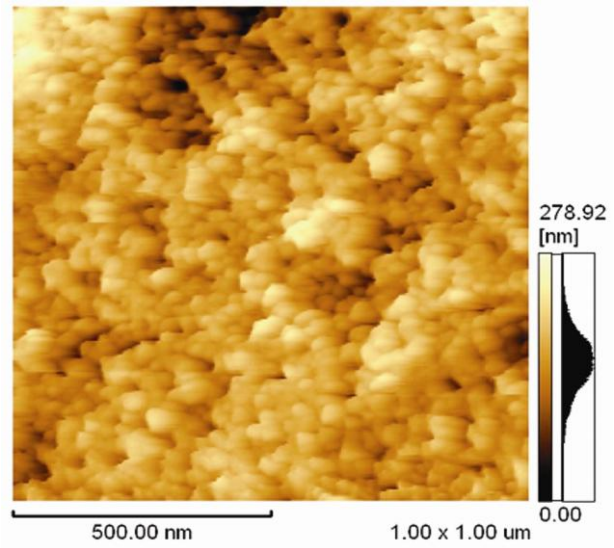

Figure 5. SPM picture (surface plot) of TiO_2 film prepared at 20 in 0.15M HF + 0.5M H_3PO_4 for 40 min. and then annealed and calcinated at 450˚C for 2 hours.

3.7. Effect of illumination

The effect of illumination on the enhancement of the conversion efficiency of TiO_2-NT_s solar cell appears clearly in Fig. 7 where TiO_2 electrode was prepared under the optimum conditions mentioned and then tested in CoPC dye in dark and under illumination of 100 mW cm^{-2}. From the results, we noticed that the photoelectrochemical response of the electrode tested under illumination (0.17%) is higher than that tested in dark (0.08%) which illustrates that the cell performance is better under illumination conditions. This might be attributed to excitation of more electrons from the ground state to the excited state in the dye which leads to the enhancement of charge separation and electron transfer processes under illumination.

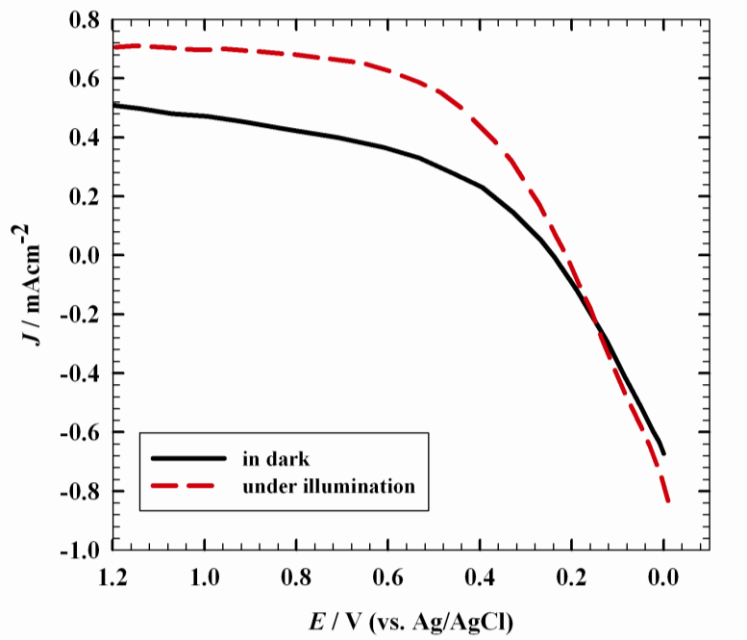

Figure 7. I-V curves of TiO_2 electrodes prepared by constant potential anodization at 20 V in 0.15M HF + 0.5M H_3PO_4 for 40 min. and then annealed and calcinated at 450˚C for 2 hours in CoPC dye electrolyte in dark and under illumination of 100 mW cm^{-2}.

The conversion efficiency values obtained in this study under optimized experimental conditions using CoPC dye and incident light intensity of 100 mW cm^{-2} is considered as a good result compared to other results mentioned in the literature.

The effect of illumination was confirmed by EIS technique. Fig. 8 shows the Nyquist plot of TiO_2 electrode prepared under optimum conditions and tested in dye solution in dark and under illumination.

Table 3 lists the best fitting values calculated from the equivalent circuit shown in Fig. 8 (the inset). The model fitted the experimental data well is shown in Fig.8 (points represent experimental data and lines represent fitted data) and provided a reliable description for the electrochemical system. From the circuit, R_s represents the electrolyte resistance, R_f and C_f represent the resistance and capacitance of TiO_2 film, R_{ct} and C_{dl} represent the charge transfer resistance and double layer

capacitance, respectively. In addition, C_{dl} was replaced with constant phase element (CPE1) in the fitting procedure due to the non-ideal capacitive response of the interface TiO_2 film/solution [31].

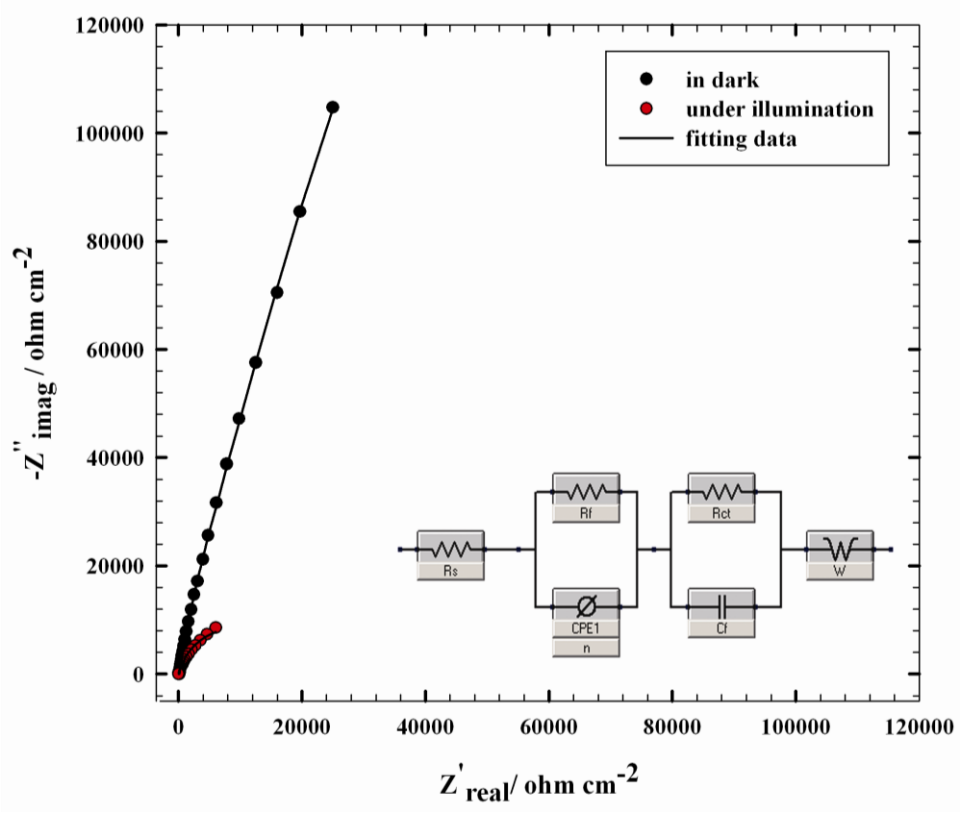

Figure 8. Nyquist plots obtained at open circuit potential for TiO_2 (prepared at 20V for 40 minutes in 0.15M HF+0.5M H_3PO_4 and annealed then calcinated at 450˚C for 2 hours) tested in dye solution in dark and under illumination. The inset is the equivalent circuit applied for fitting of experimental data.

Table 3. The electrochemical parameters, corresponding to Fig. 8, estimated from the fitting of experimental data to the equivalent circuit shown as the inset of Fig. 8.

TiO_2 electrode	R_s / Ω cm^{-2}	R_f / Ω cm^{-2}	CPE_1/ F cm^{-2}	n	R_{ct} / Ω cm^{-2}	W/ Ω $s^{-1/2}$	C_f/ F cm^{-2}
In dark	**121**	**1.8×10^4**	**2.3×10^4**	**0.83**	**8.4×10^5**	**1.9×10^2**	**1.5×10^{-5}**
Under illumination	**16**	**1.3×10^3**	**4.5×10^3**	**0.82**	**1.6×10^4**	**5.4×10^{-2}**	**8.9×10^{-5}**

The following conclusions could be drawn from EIS data:

- Resistance-capacitance (RC) arcs were observed. These arcs were associated with the properties of the TiO_2 films. The arc radius corresponded to the resistance (R_{ct}) of electrons

transferring through the TiO_2 film. The RC arcs shrank remarkably, the diameter of the semicircle was decreased and R_{ct} was decreased under illumination compared with those in dark implying that illumination increased the capacitance and decreased the resistance to Faraday current [32]. This could be attributed to the different distribution and density of the electrons under illumination and non-illumination.

- Lower impedance usually means better charge transfer and electronic conductivity for dye-TiO_2/Ti nano-composite electrode, i.e., better conversion efficiency of the electrode. Such an ordered arrangement of nanotubular channels ultimately contributed to prompting electron shift as well as photosensitivity in the photoelectrochemical process [33]. This result agrees with the data obtained from I-V curves.
- For the electrode with a TiO_2 semiconductor film, the carriers on the electrode only originated from thermodynamic excitation under dark condition, so the Faraday current was very weak, correspondingly exhibiting an extremely high R_{ct}. However, when the TiO_2 film was illuminated, a large number of photogenerated carriers accumulated and moved toward one direction under the action of space charge electric field in addition to the thermodynamically excited carriers, resulting in the tremendous increase in the concentration of electrons and consequently the Faraday current in the electrode. As a result, the R_{ct} of the semiconductor TiO_2 film decreased significantly.
- It is interesting that two RC arcs were seen for TiO_2 under the conditions of irradiation and non-irradiation, implying that the reaction at the interface of Ti/solution was controlled by two time constants [32]. Laser et al. [34] reported that the natural passive film on the titanium surface was semi-conductive. Thus, the arc in the lower frequency could be related to the inner dense passive layer, and the RC arc in the higher frequency range reflected outer loose TiO_2 layer.

3. CONCLUSIONS

Nanotubular TiO_2 can be formed in a very controlled way by electrochemical anodization in aqueous phosphoric acid solution containing hydrofluoric acid. TiO_2-NT_s arrays were employed as photoanodes for dye sensitized solar cells ($DSSC_s$) using metal phthalocyanine dyes. The factors affecting morphology and crystal phase behavior of TiO_2-NT_s were studied in order to achieve the optimum conditions for TiO_2 electrode that shows the greatest photoelectrochemical response of $DSSC_s$. Cell voltage anodization controls the pore diameter of TiO_2-NT_s where a cell voltage of 20 V shows the largest pore diameter (110 nm) and the best conversion efficiency percent (0.16%) under illumination. Hydrofluoric acid plays a major role in pore formation and dissolution. Steady state nanotubular formation is possible when the mole fraction of HF used is around 0.23. Calcination conditions affect strongly the morphology and crystallographic structure of TiO_2-NT_s. It was found that the electrode examined without calcination does not contain TiO_2 but Ti is only present. Better conversion efficiency values were obtained when TiO_2 was calcinated at 450˚C for 2 hours. The dye used in DSSC improves strongly its performance and efficiency. CoPC dye showed better conversion efficiency under illumination of 100 mW cm^{-2} (0.17%) compared to dark conditions (0.08%). The

effect of illumination on enhancement of the photoelectrochemical behavior of TiO_2-NT_s electrode was explained and confirmed by electrochemical impedance spectroscopy technique.

ACKNOWLEDGMENT
The authors would like to acknowledge the financial support from Cairo University through the Vice President Office for Research Funds.

References

1. B.O'Regan, M.Grätzel, *Nature* 353 (1991) 737-740.
2. Y.C.Hsu, H.Zheng, J.T.Lin, K.C.Ho, *Sol. Energy Mater. Sol. Cells* 87 (2005) 357-367.
3. L.Y.Liang, S.Y.Dai, L.H Hu, F.T.Kong, W.W.Xu, K.J.Wang, *J. Phys. Chem*. B 110 (2006) 12404–12409.
4. X.Pan, S.Y.Dai, K.J.Wang, L.H.Hu, C.W.Shi, L.Guo, F.T.Kong, *Chin. J. Chem*. 23 (2005) 1579–1583.
5. D.Cahen, G.Hodes, M.Gratzel, J.F.Guillemoles, I.Riess, *J. Phys. Chem*. B 104 (2000) 2053–2059.
6. J. Nowotny,T.Bak,M.K.Nowotny, L.R.Sheppard, *Int. J.Hydrogen Energy* 32 (2007) 2609-2629.
7. Y.Xu, Z.Z.Zhu, W.Chen, G.Ma, *Chin. J. Appl. Chem*. 8 (1991) 28-32.
8. K.Wilke, H.D. Breuer, *J.Photochem. Photobiol*., A 121 (1999) 49-53.
9. K.-M. Lee,V. Suryanarayanan, K.-C. Ho, *J. Power Sources* 188 (2009) 635-641.
10. B.Liu, E.S.Aydil, *J.Am. Chem. Soc*. 131 (2009) 3985-3990.
11. F.M. Bayoumi, B.G.Ateya, *Electrochem. Commun*. 8 (2006) 38-46.
12. D.Eder, M.S. Motta, I.A. Kinloch, A.H. Windle, *Physica* E 37 (2007) 245-249.
13. Z.-Y. Yuan, B.-L. Su, *Colloid Surf. A: Physicochem. Eng. Asp*. 241 (2004) 173-183.
14. F.M.B.Hassan, H.Nanjo, M.Kanakubo, I.Ishikawa, M.Nishioka, *J.Surf.Sci. Nanotech*. 7 (2009) 84-88.
15. S.Baea, E.Shimb, J.Yoonc, H Joo, *J.Power Sources* 185 (2008) 439-444.
16. M.S.Akhtar, J.M.Chun, O.B.Yang, *Electrochem. Commun*. 9 (2007) 2833-2837.
17. Y.Xie. *Electrochim. Acta* 51 (2006) 3399-3406.
18. Z.Wu, S.Guo, H.Wang, Y.Liu, *Electrochem. Commun*.11 (2009) 1692-1704.
19. P.Sudhagar, R.Sathyamoorthy , S.Chandramohan, *Appl. Surf. Sci*. 254 (2008) 1919-1928.
20. M.V.Diamanti, M.P.Pedeferri. *Corros. Sci*. 49 (2007) 939-948.
21. A.L.Thomas, Ed. ''Phthalocyanine Research and Applications, CRC Press, Boston, 1990.
22. M.K.Nazeeruddin, R.Humphry-Baker, M.Grätzel, B.A.Murrer, *Chem. Commun*. (1998) 719-720.
23. S.K.Mohapatra, M.Misra, V.K.Mahajan, K.S.Raja. *J. Catal*. 246 (2007) 362-369.
24. M.Bestetti, S.Franz, M.Cuzzolin, P.Arosio, P.L.Cavallotti, *Thin Solid Films* 515 (2007) 5253-5258.
25. N.R.de Tacconi, C.R.Chenthamarakshan, G.Yogeeswaran, A.Watcharenwong, R.S. de Zoysa, N.A.Basit, K.Rajeshwar, *J. Phys. Chem*. B 110(2006)25347-25355.
26. Young-Taeg Sul, C.B.Johansson, Y.Jeong, T.Albrektsson, *Med. Eng. Phys*. 23 (2001) 329-346.
27. G.K.Mor,O.K.Varghese, M.Paulose, K.Shankar, C.A.Grimes, *Sol. Energy Mater. Sol. Cells* 90 (2006) 2011-2075.
28. L.S.Mende, M.Grätzel, *Thin solid films* 500 (2006) 296-301.
29. Allen J.Bard, Larry R.Faulkner, "Electrochemical Methods, Fundamentals and Applications", second edition, chapter 12, John Wiley & Sons, 2001
30. Z.Zhang, Y.Yuan, L.Liang, Y.Cheng, H.Xu, G.Shi, L.Jin, *Thin Solid Films* 516 (2008) 8663-8667.
31. M.C.Li, C.L.Zeng, S.Z. Luo, J.N.Shen, H.C.Lin, C.N.Cao, *Electrochim. Acta* 48 (2003) 1735-1741.
32. Z.Li, Z.Pengyi, C.Songzhe, *Chin. J. Catal*. 28(2007) 299-306.

33. Y.Xie, L.Zhou, H.Huang, *J.Lu, Composites: Part A* 39 (2008) 690-696.
34. D.Laser, M.Yaniv, S.Gottesfeld, *J.Electrochem. Soc*., 125 (1978) 358-360.